

Phase problem and the Radon transform

Andrei V. Bronnikov

Bronnikov Algorithms
The Netherlands

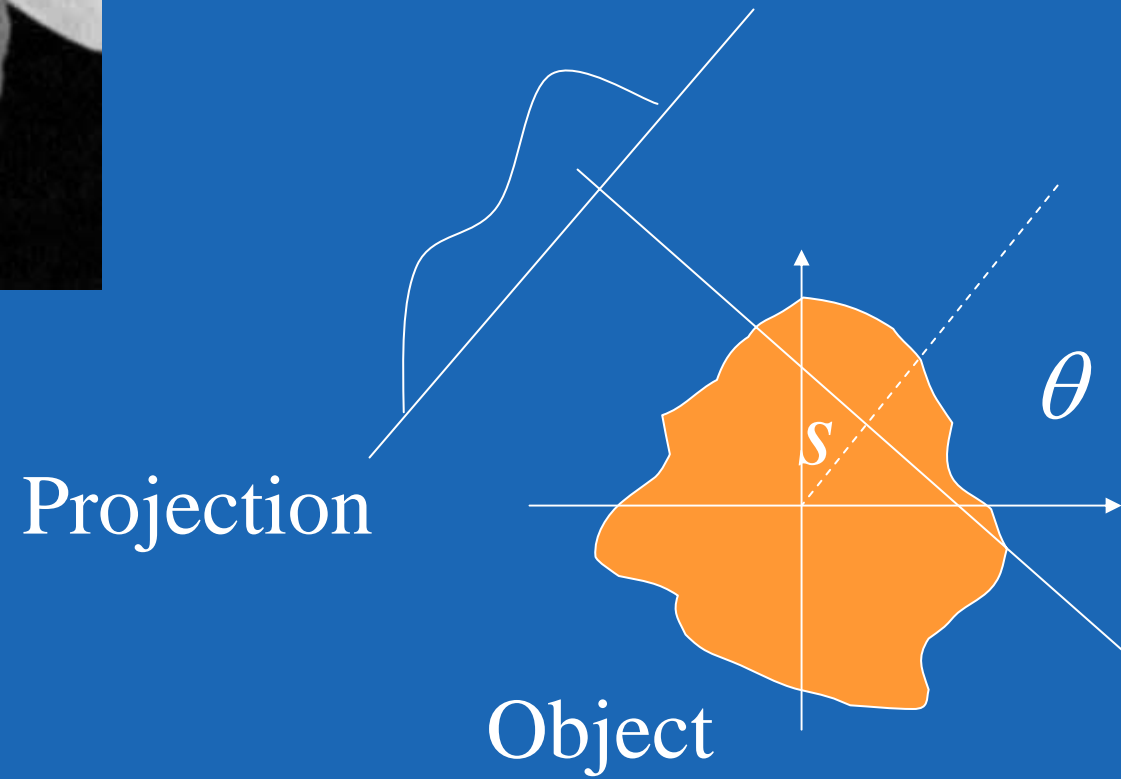
- The Radon transform and applications
- Inverse problem of phase-contrast CT
- Fundamental theorem
- Image reconstruction algorithms
- Phantom studies
- Experimental data

The Radon transform (J. Radon, 1917)



$$\hat{f}_{\theta,s} = \int f \, dl$$

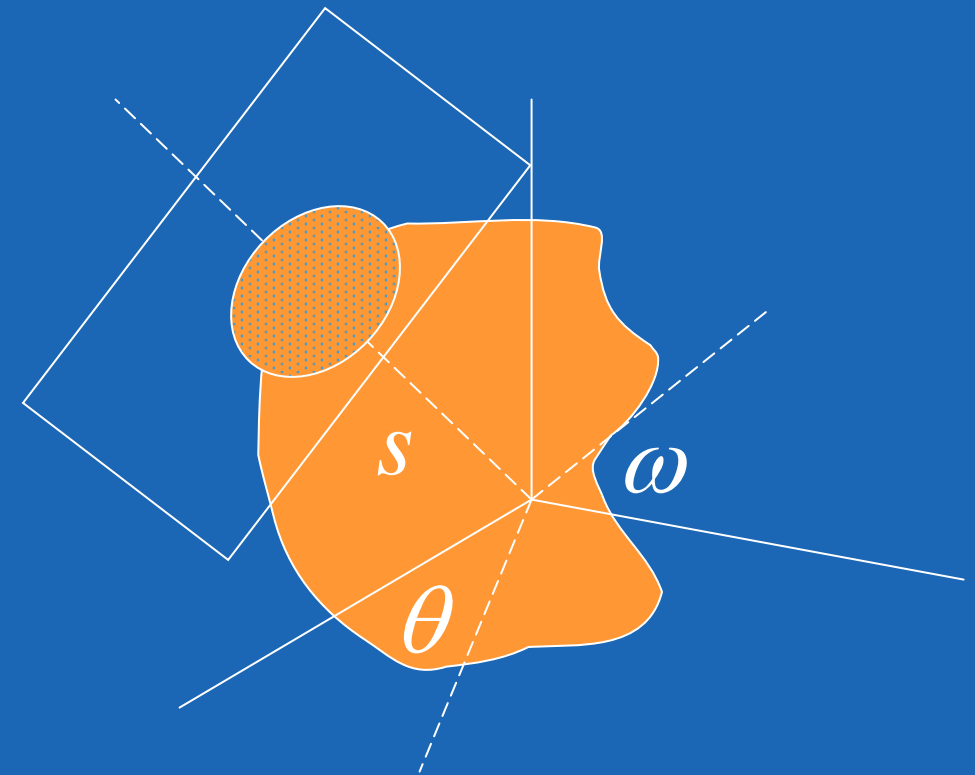
Line (θ,s)



The inverse 3D (Radon) transform (H.A. Lorentz, 1905)

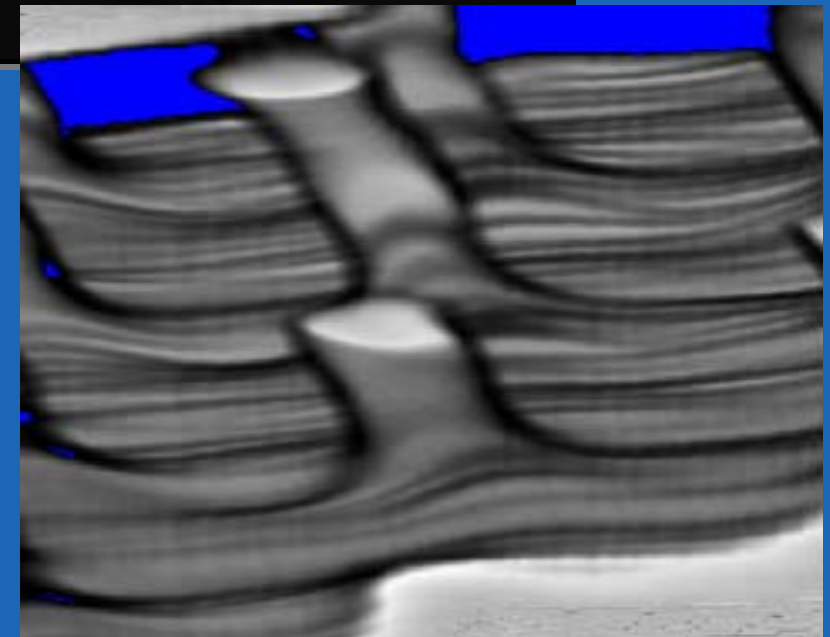
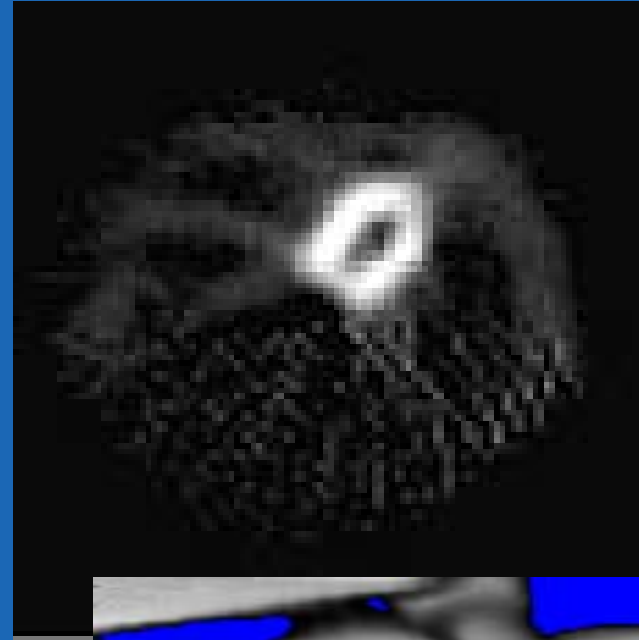


$$f = \frac{-1}{4\pi^2} \iint \frac{\partial^2}{\partial s^2} \hat{f}(s, \theta, \omega) d\theta d\omega$$

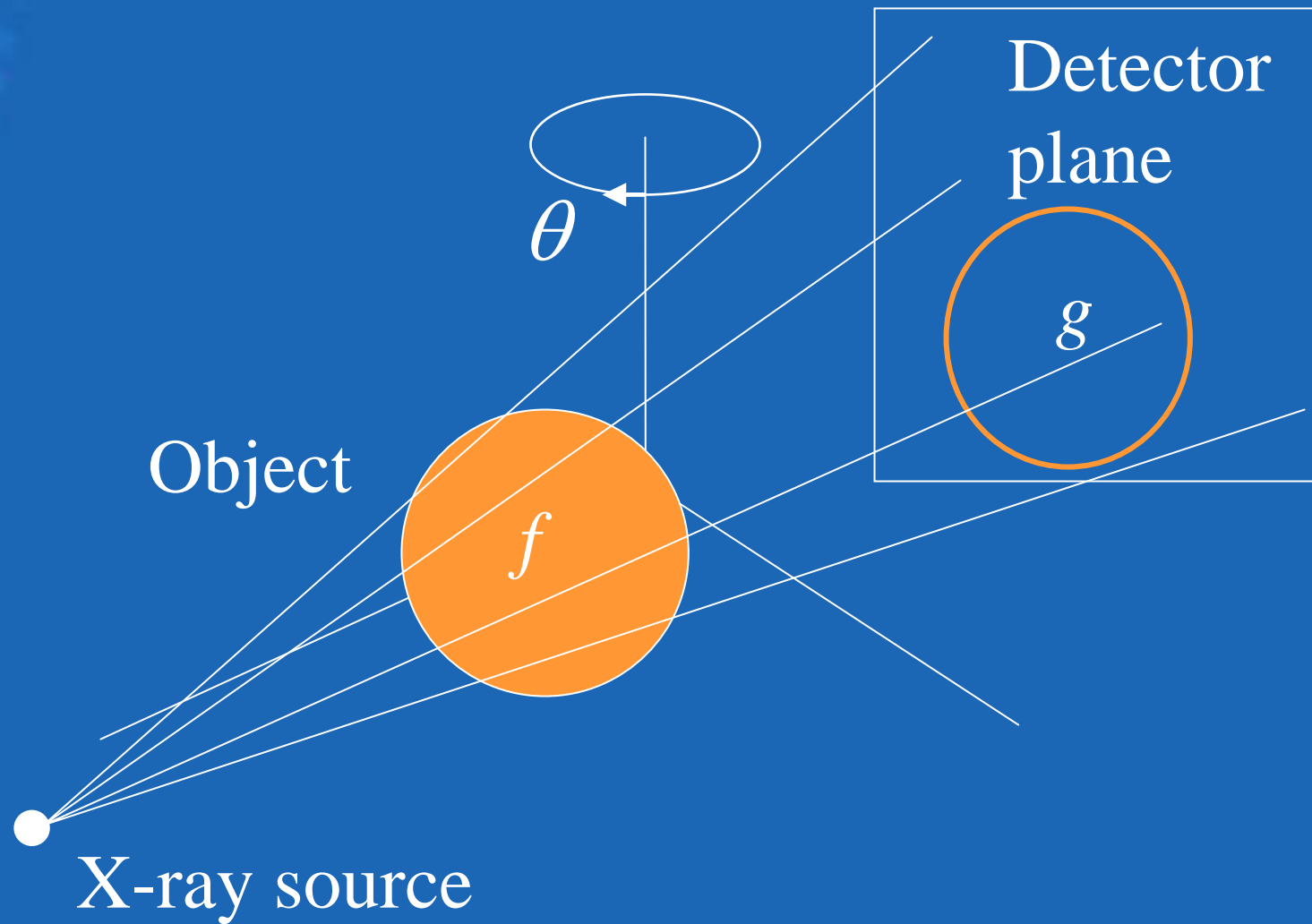


Applications

- Medical imaging
- Laboratory animals
- Materials research
- Non-destructive testing
- Reverse engineering
- Geophysics



Principle of x-ray tomography



Fourier slice theorem

$$\hat{f}(u_\theta, v_\theta) = \hat{g}_\theta(u, v)$$

Fourier transform in the central plane
is the Fourier transform of the
projection

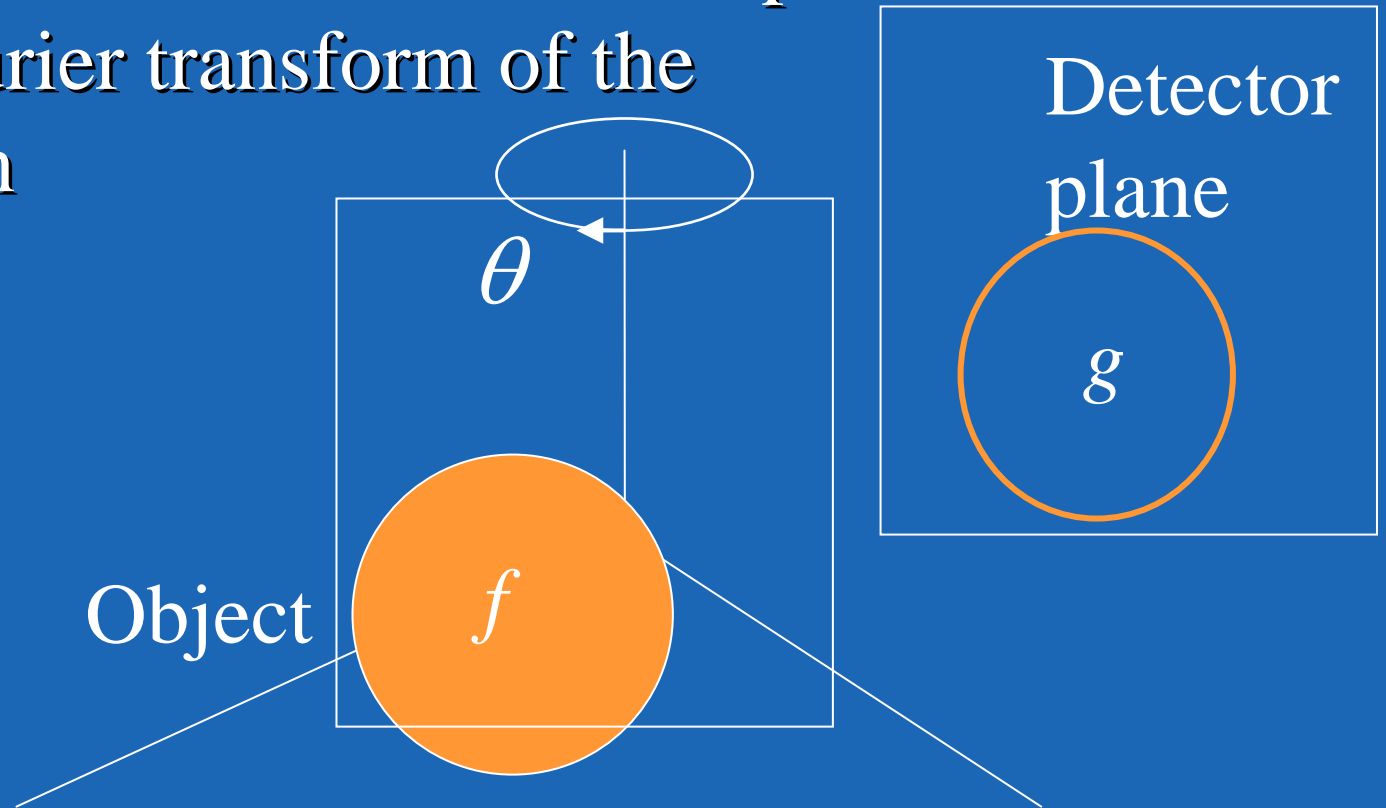
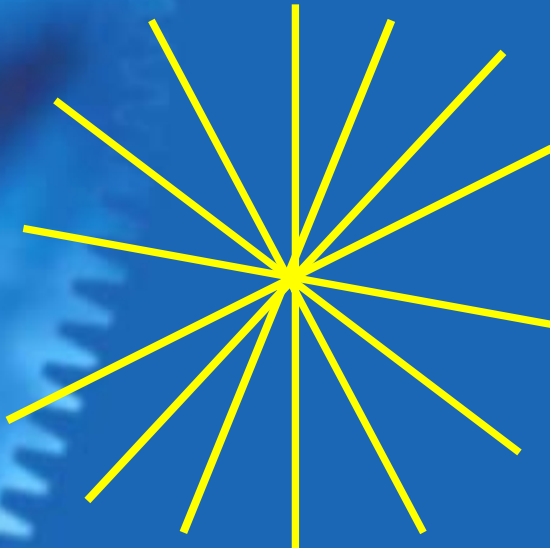


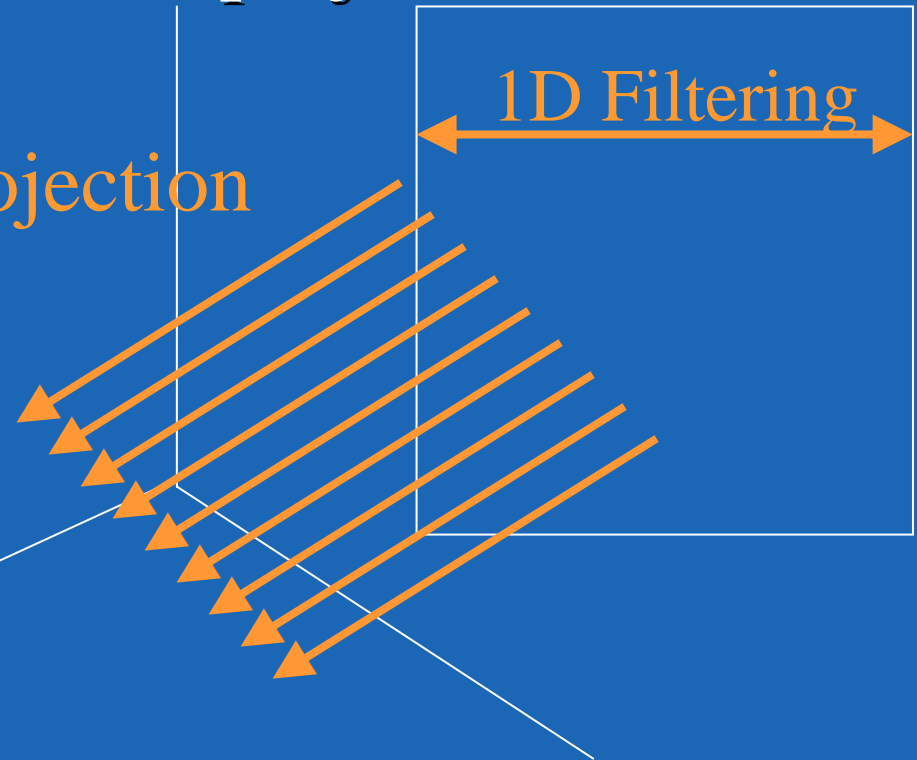
Image reconstruction



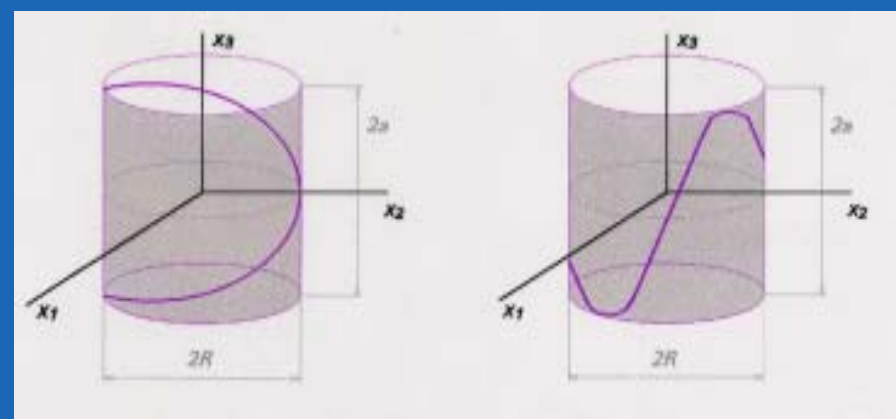
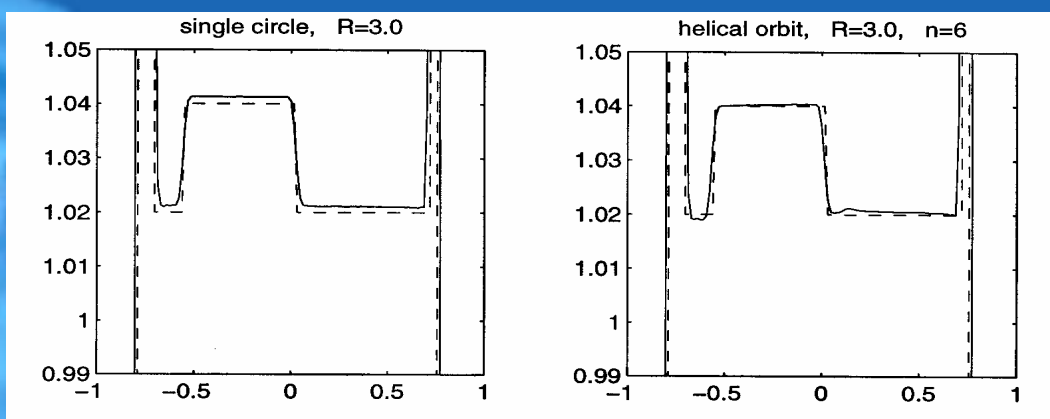
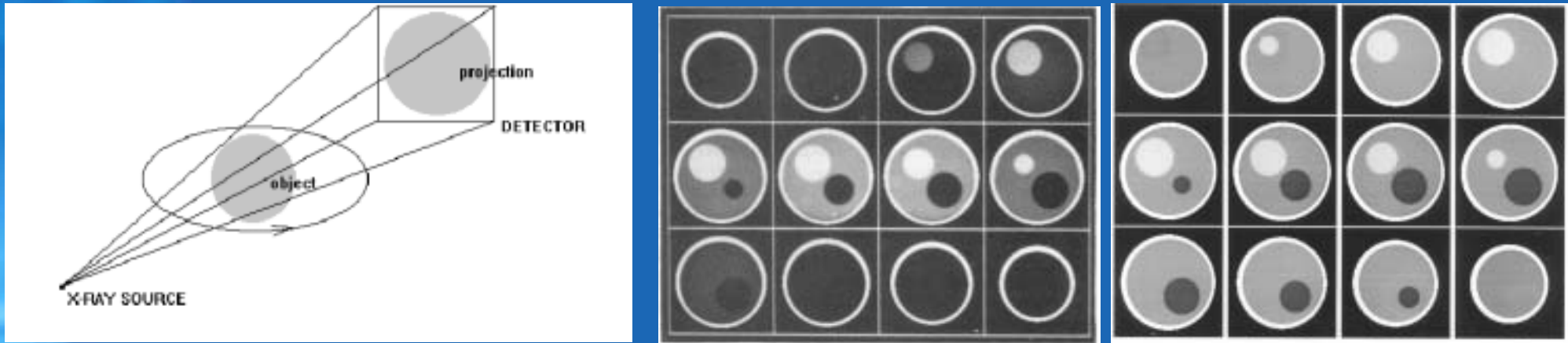
- Filling up the Fourier space
- Filtered backprojection:

$$f = \int_0^{\pi} q * g_{\theta} d\theta$$

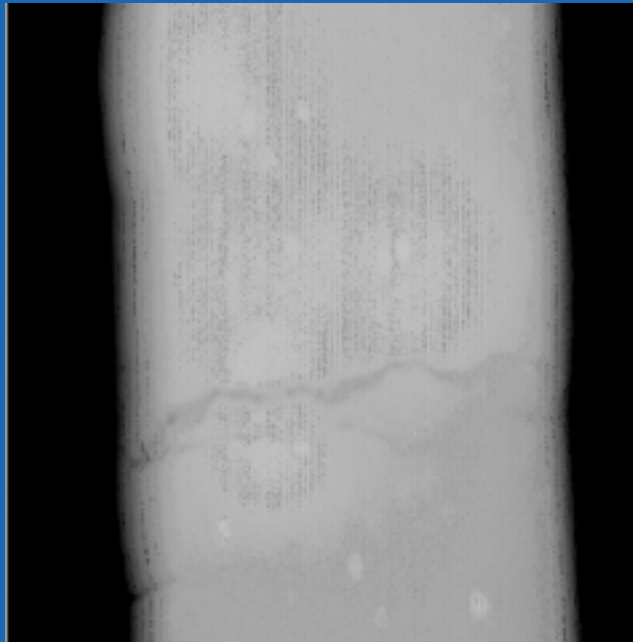
Backprojection



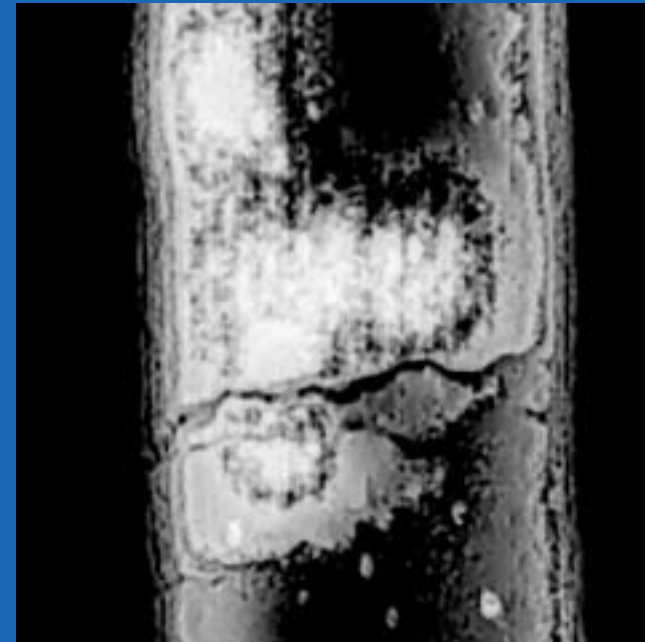
Density reconstruction; non-planar orbits (Bronnikov, 1995-2002)



Wavelet-based contrast enhancement



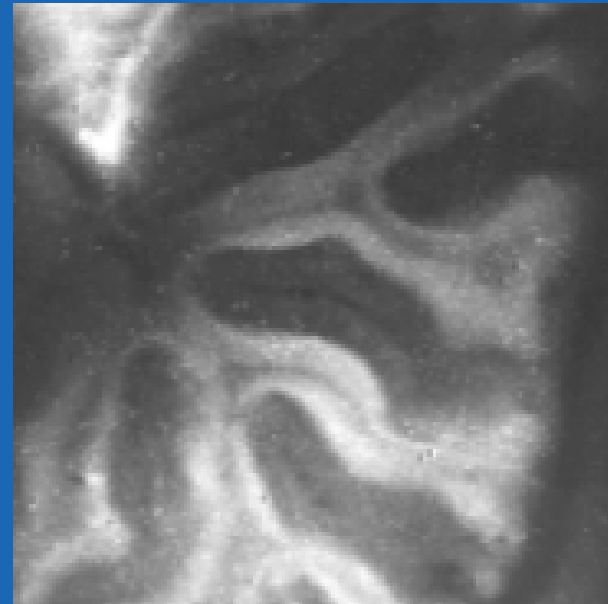
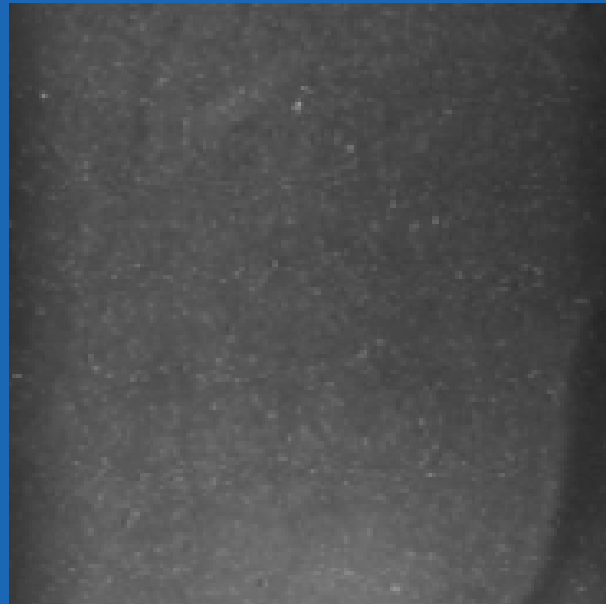
Original image



Processed image

Bronnikov and Duifhuis, 1998

Contrast-enhanced imaging



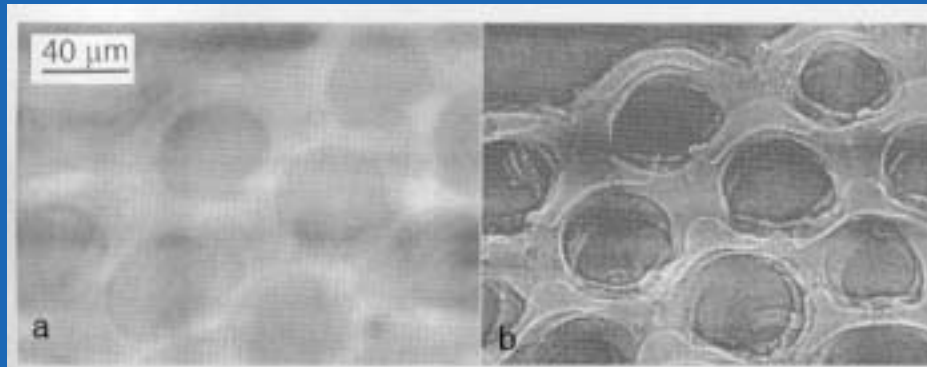
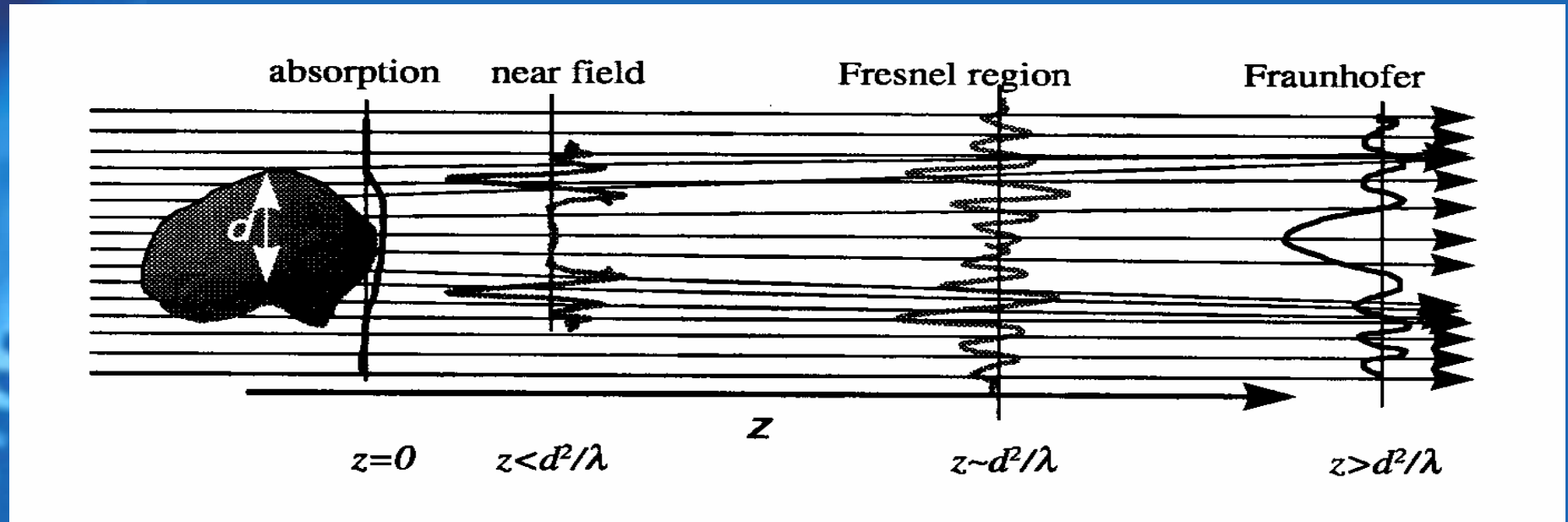
X-ray images of the rat cerebellum

Absorption contrast

Phase contrast

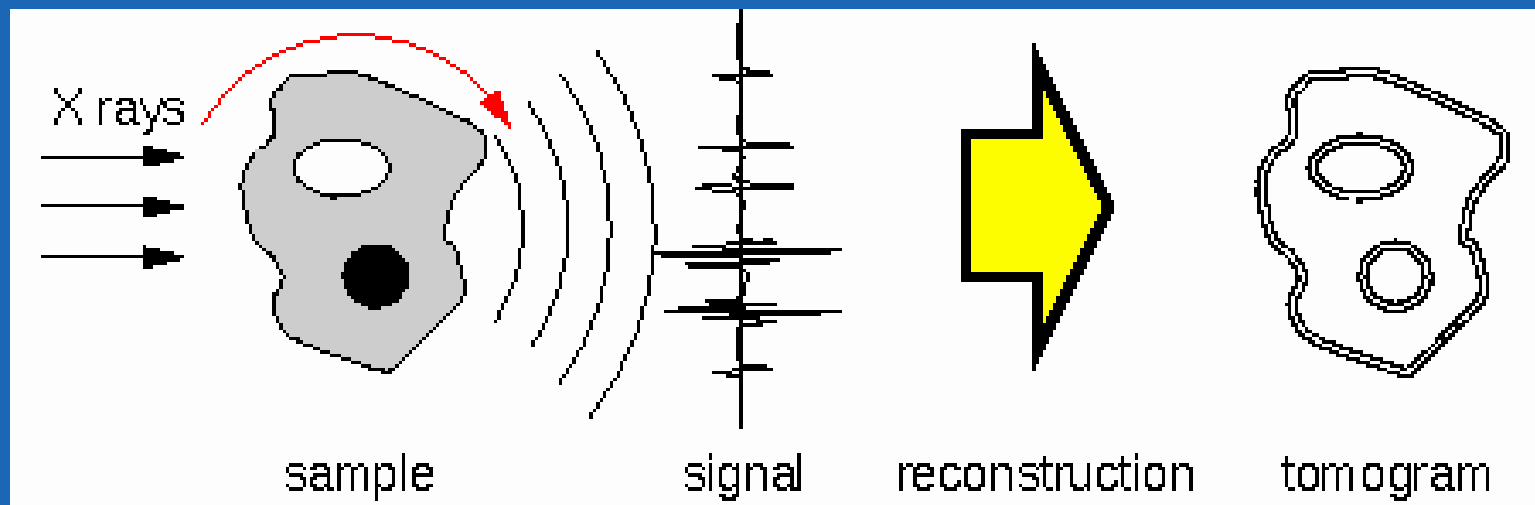
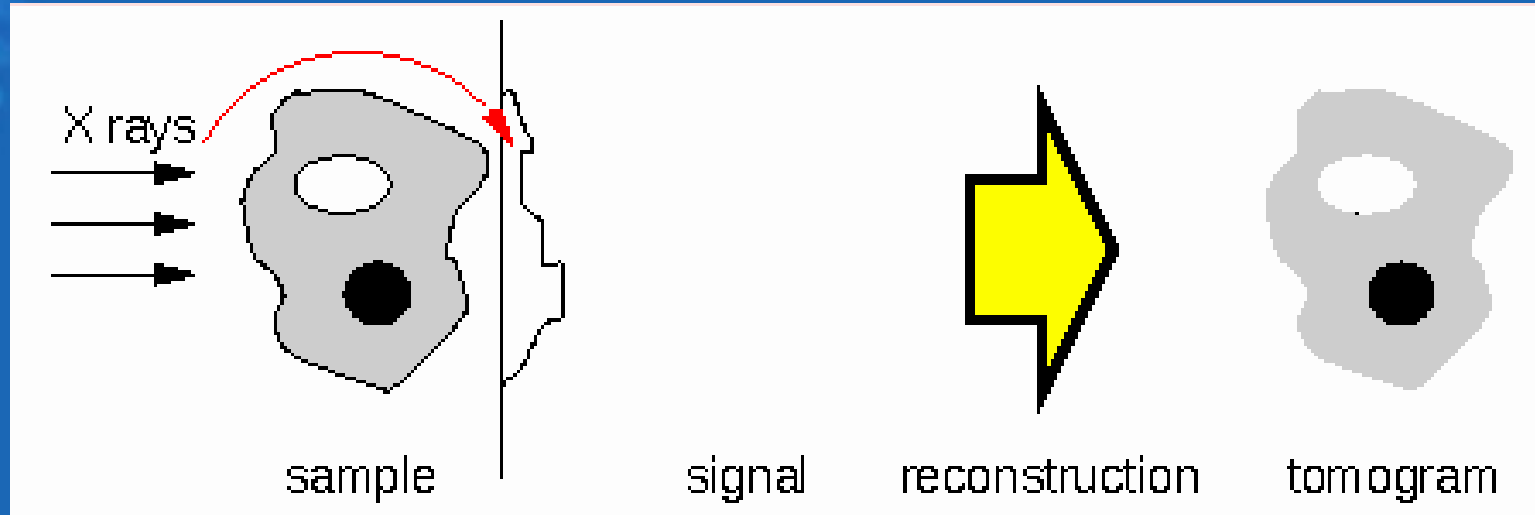
A. Momose, T. Takeda, Y. Itai and K. Hirao, *Nature Medicine*, 2, 473-475 (1996).

Phase-contrast imaging



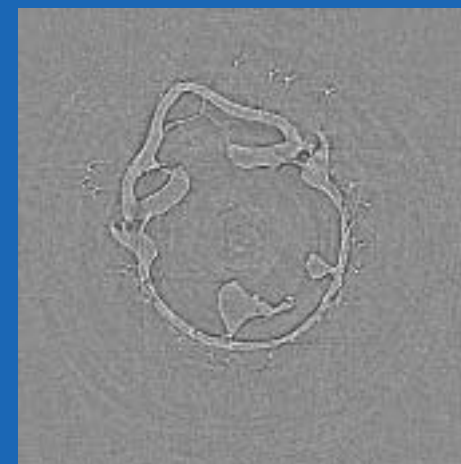
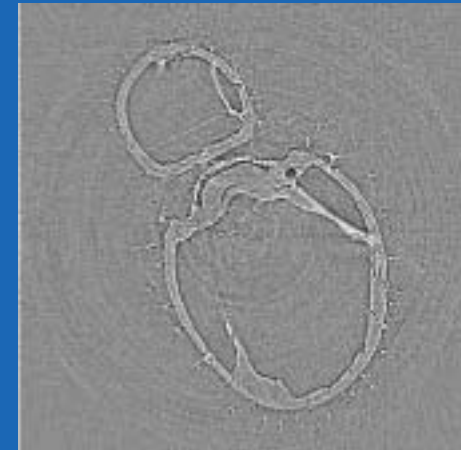
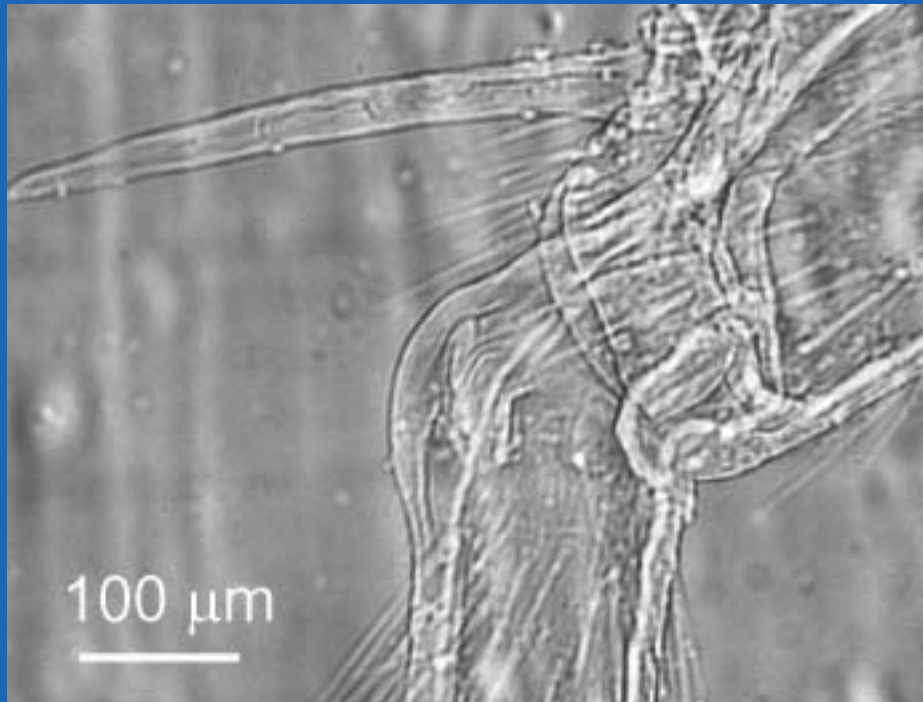
- Coherent x-rays
- Microfocus tube

Phase-contrast CT vs. absorption-contrast CT (ESRF)



Insect knee E=18 KeV

Snigirev et al, ESRF



Problems

- the lack of the linear theory comparable to that of conventional absorption-based CT
- no quantitative solution (only edges of the objects are reconstructed)
- huge amount of high-resolution data

Goals

- to develop an accurate and practical mathematical tool for quantitative phase-contrast **image** reconstruction
- to suggest the fastest image reconstruction algorithm for phase-contrast CT

Inverse problem of phase-contrast tomography

find $f(x_1, x_2, x_3)$ from $I_\theta^z(x, y), 0 \leq \theta < \pi$

- Phase retrieval (holographic) approach
(Cloetens et al 1999):
 - find the phase from intensity
 - invert Radon transform to reconstruct the object
- Reconstruction formula (CT approach):
 - a straightforward linear relation between the intensity and the object function

Phase retrieval

- Nonlinear iterative methods
(Gershberg, Saxton 1972; Fienup, 1982)
- Linear TIE method (Gureyev et al, 2004)
- Linear Wigner transform (Maier,
Preobrazshenski 1990; Raymer et al 1994)

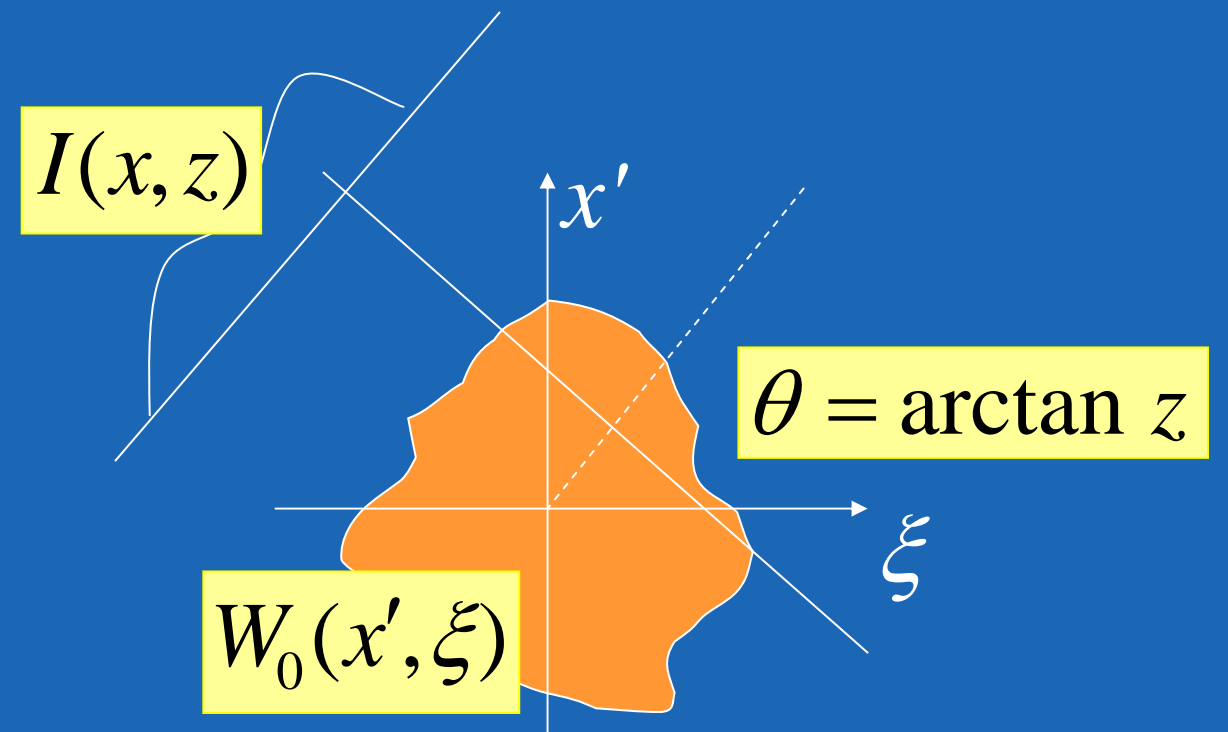
Wigner transform

$$W_z(x, \xi) = \int_{-\infty}^{\infty} \left\langle V_z^*(x - \frac{x'}{2}) V_z(x + \frac{x'}{2}) \right\rangle e^{-2\pi i \xi x'} dx'$$

$$\begin{array}{ccc} \text{Radon transform} & & \text{Inverse Wigner} \\ I(x, z) & \Rightarrow & W_0(x, \xi) \\ & & \Rightarrow \\ & & V_0^*(x) V_0(0) \Rightarrow \varphi(x) \end{array}$$

Radon-Wigner transform

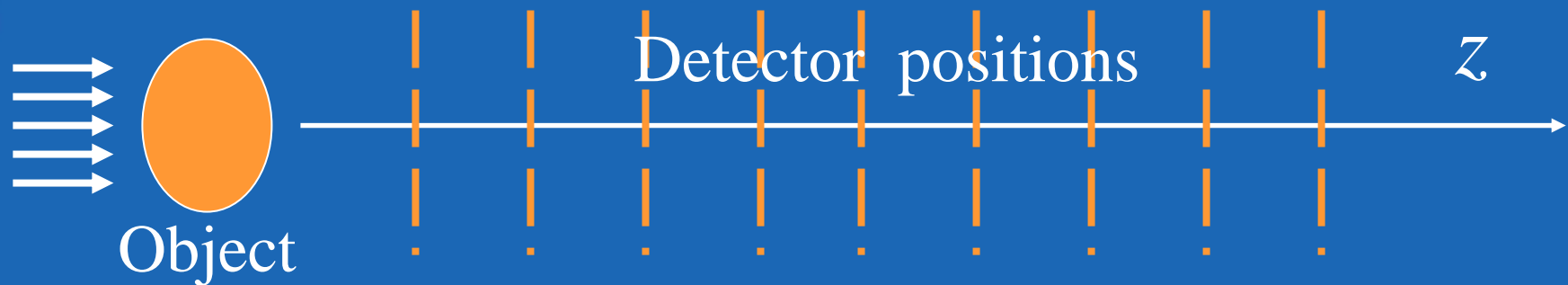
$$\int_{-\infty}^{\infty} \int_{-\infty}^{\infty} W_0(x', \xi) \delta(x - z\xi - x') dx' d\xi = I(x, z)$$



Implementation (Bronnikov et al 1991)

n - number of samples of the discrete Wigner function

$$\text{Number of detection planes} \geq \frac{\pi n}{2}$$



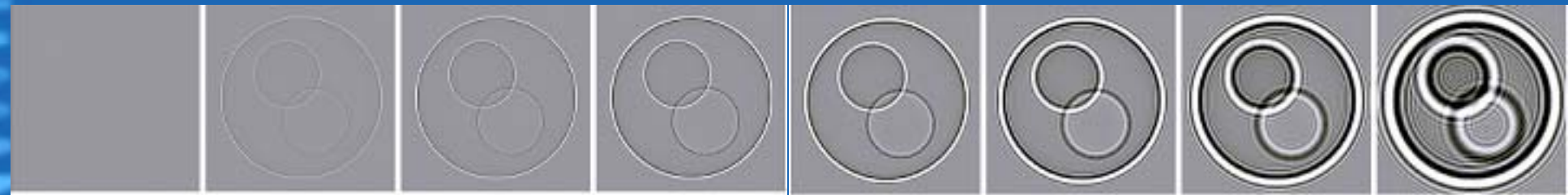
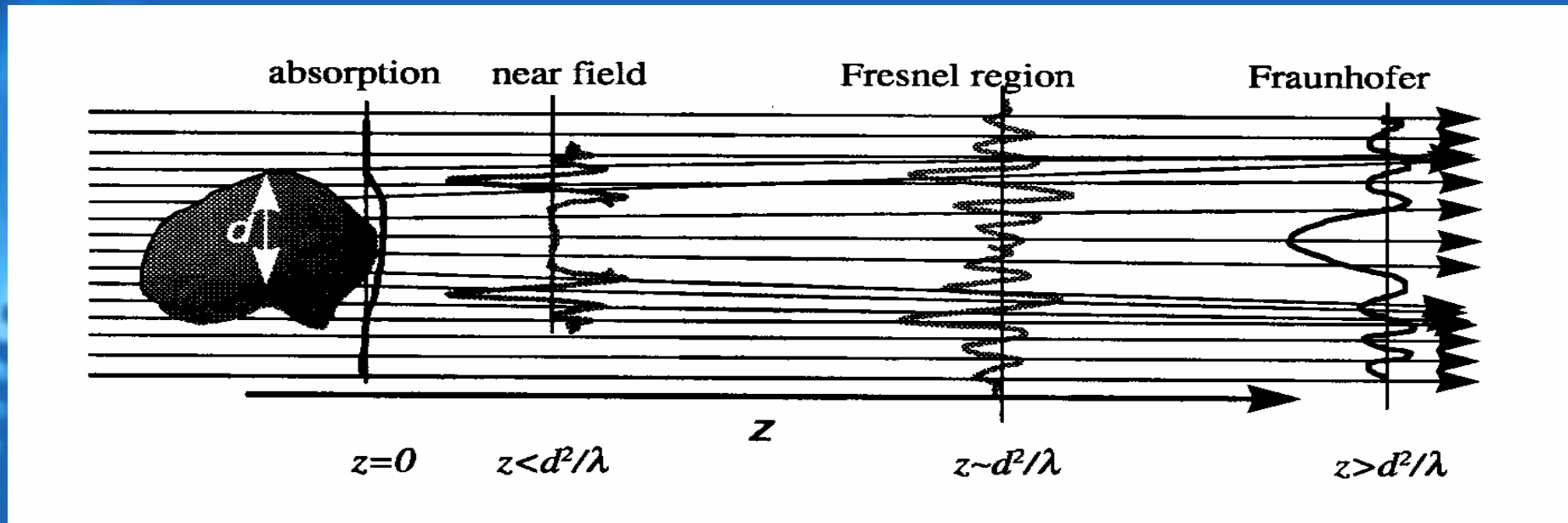
$$I(x, z) \xrightarrow{\text{Radon transform}} W_0(x, \xi) \xrightarrow{\text{Inverse Wigner}} V_0^*(x)V_0(0) \Rightarrow \varphi(x)$$

Inverse problem of phase-contrast tomography

find $f(x_1, x_2, x_3)$ from $I_\theta^z(x, y), 0 \leq \theta < \pi$

- Phase retrieval (holographic) approach:
 - find the phase from intensity
 - invert Radon transform to reconstruct the object
 - multiple detector positions along the beam
- Reconstruction formula (CT approach):
 - a straightforward linear relation between the intensity and the object function
 - single detector position

Mathematical model: the Fresnel propagator



Theoretical background

$$T_\theta(x, y) = e^{-\frac{1}{2}\mu_\theta(x, y) + i\varphi_\theta(x, y)}$$

Transmission function

$$U_\theta(x, y) = T_\theta(x, y) U_i$$

Wavefield

$$I_\theta^z(x, y) = |h_z \ast \ast U_\theta|^2, \quad 0 \leq \theta < \pi$$

Fresnel propagation

$$\lambda d < D^2 \quad \left| \frac{\partial \mu_\theta}{\partial x} \right|, \left| \frac{\partial \mu_\theta}{\partial y} \right| \rightarrow 0$$

Conditions

$$I_\theta^d(x, y) = I_\theta^0 \left[1 - \frac{\lambda d}{2\pi} \nabla^2 \varphi_\theta(x, y) \right]$$

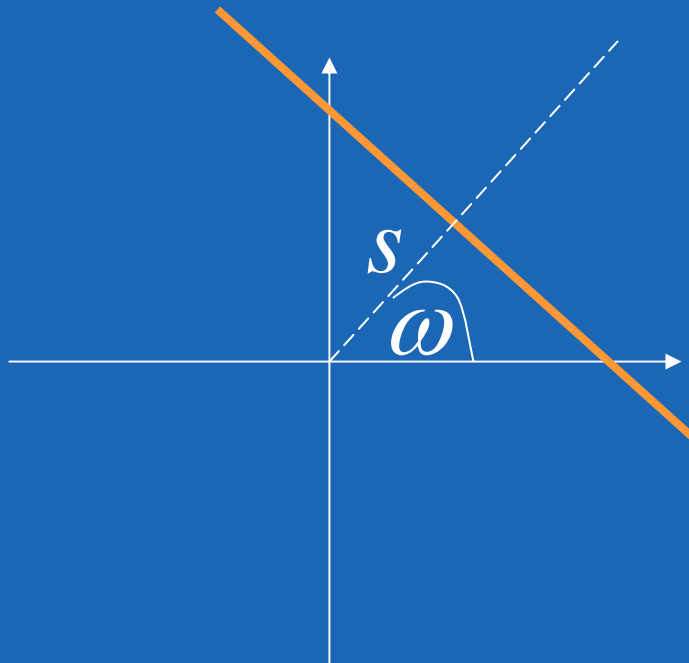
Intensity equation

Radon transforms

2D transform (lines)

$$\hat{f}_{\omega,s} = \int f \, dl$$

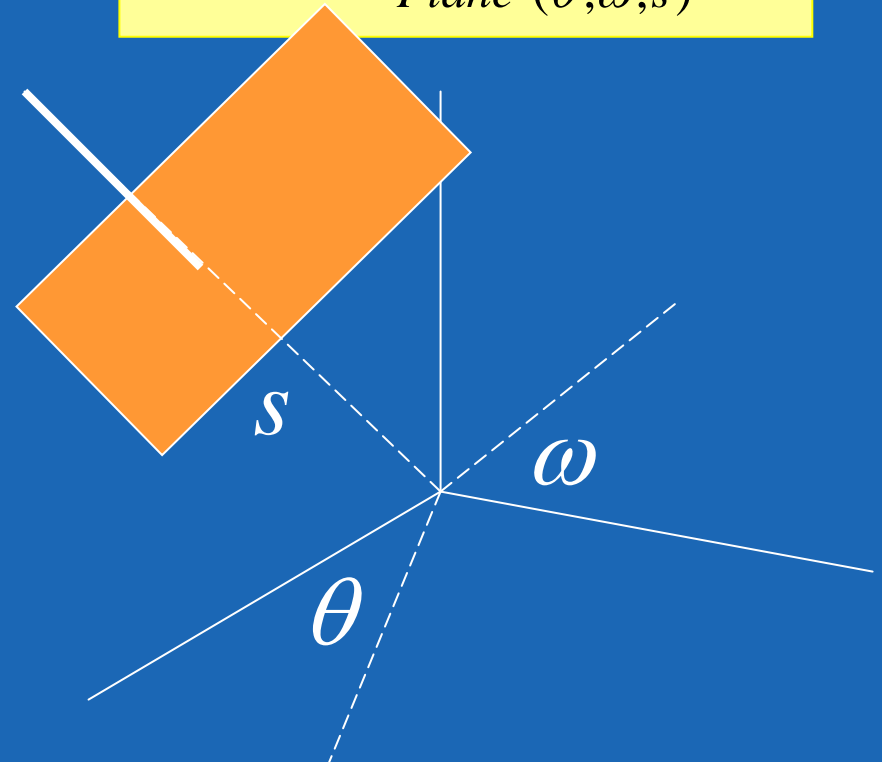
Line (ω, s)



3D transform (planes)

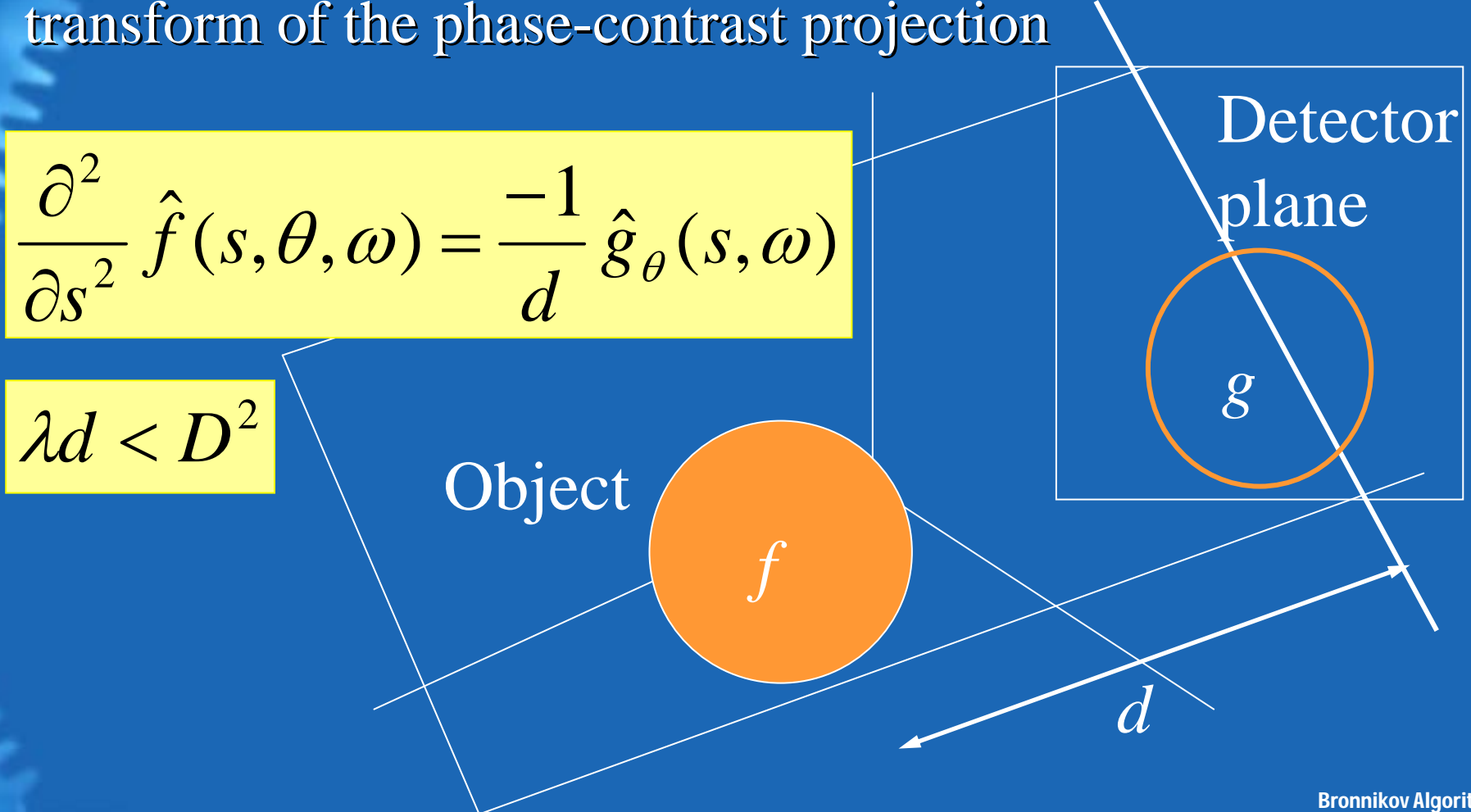
$$\hat{f}_{\theta,\omega,s} = \int f \, d\sigma$$

Plane (θ, ω, s)



Fundamental theorem (Bronnikov 2002)

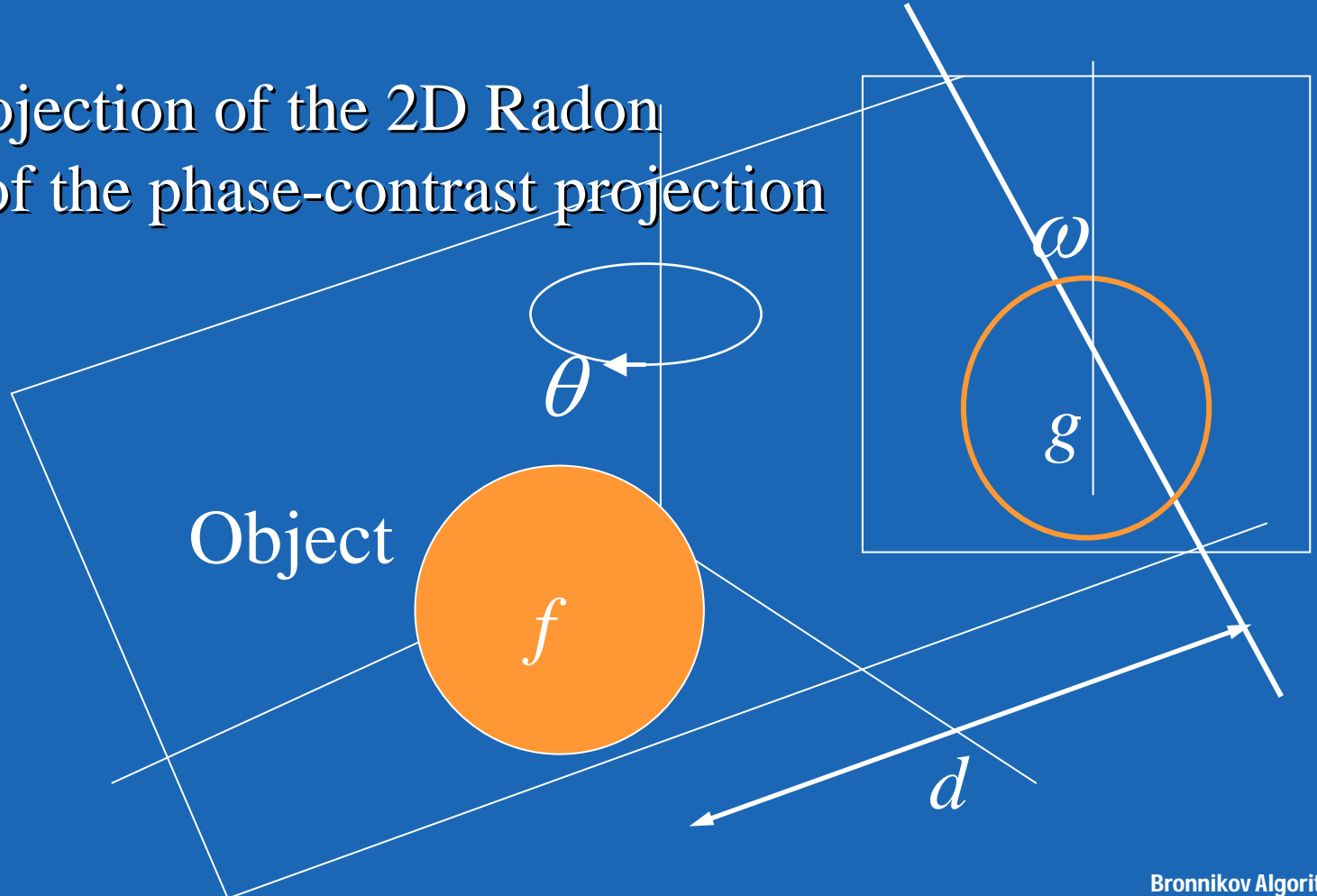
Second derivative of 3D Radon transform of the object is proportional to 2D Radon transform of the phase-contrast projection



Inversion formula (Bronnikov 1999)

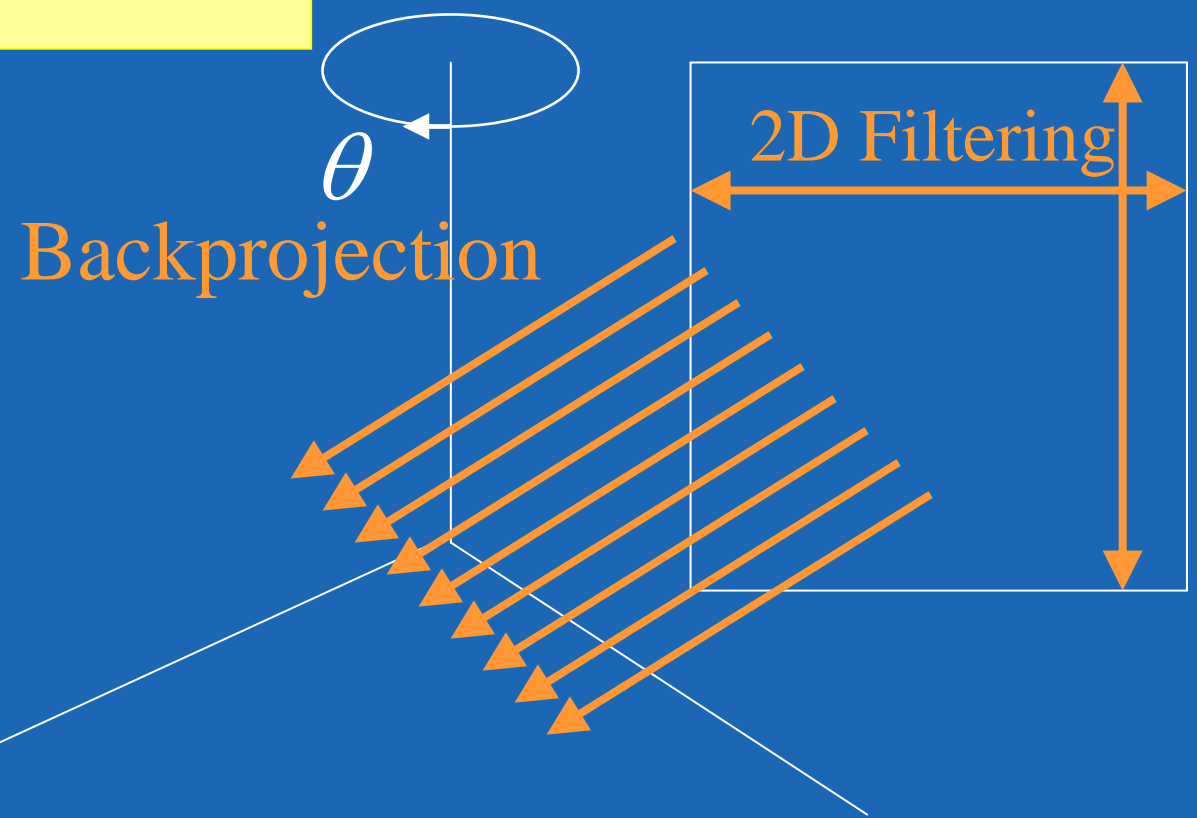
$$f = \frac{-1}{4\pi^2} \iint \frac{\partial^2}{\partial s^2} \hat{f}(s, \theta, \omega) d\theta d\omega = \frac{1}{4\pi^2 d} \iint \hat{g}_\theta(s, \omega) d\theta d\omega$$

3D backprojection of the 2D Radon transform of the phase-contrast projection

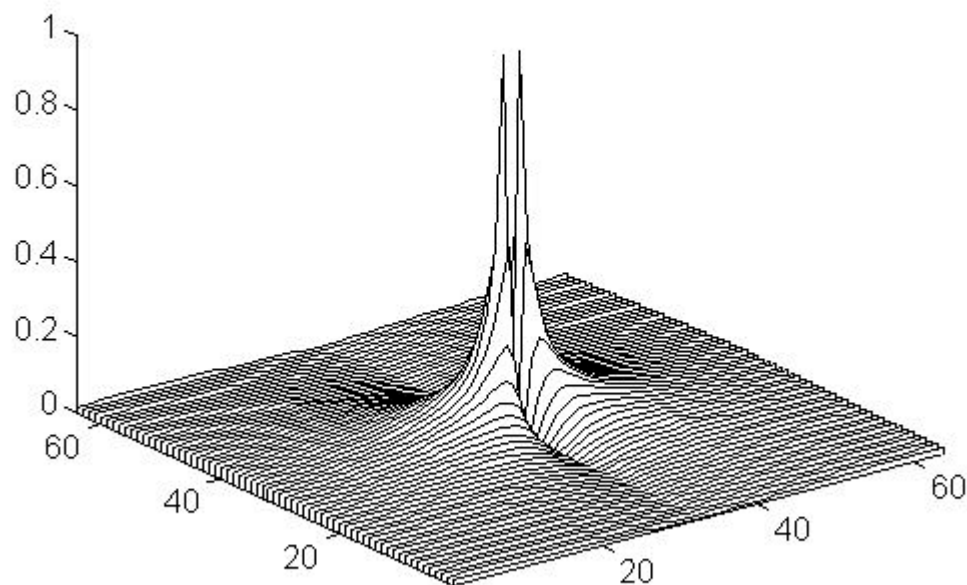


FBP algorithm (Bronnikov 1999, 2002)

$$f = \frac{1}{4\pi^2 d} \int_0^\pi q ** g_\theta d\theta$$



Analytical filter function (Bronnikov 1999, 2002)



$$f = \frac{1}{4\pi^2 d} \int_0^\pi q^{**} g_\theta d\theta$$

$$q = \frac{|y|}{x^2 + y^2}$$

MTF of the 2D filter:

$$Q = \frac{|\xi|}{\xi^2 + \eta^2}$$

Implementation

- FFT-based linear filtering
- 2D parallel-beam backprojection
- FBP structure (parallelization)
- Hardware acceleration

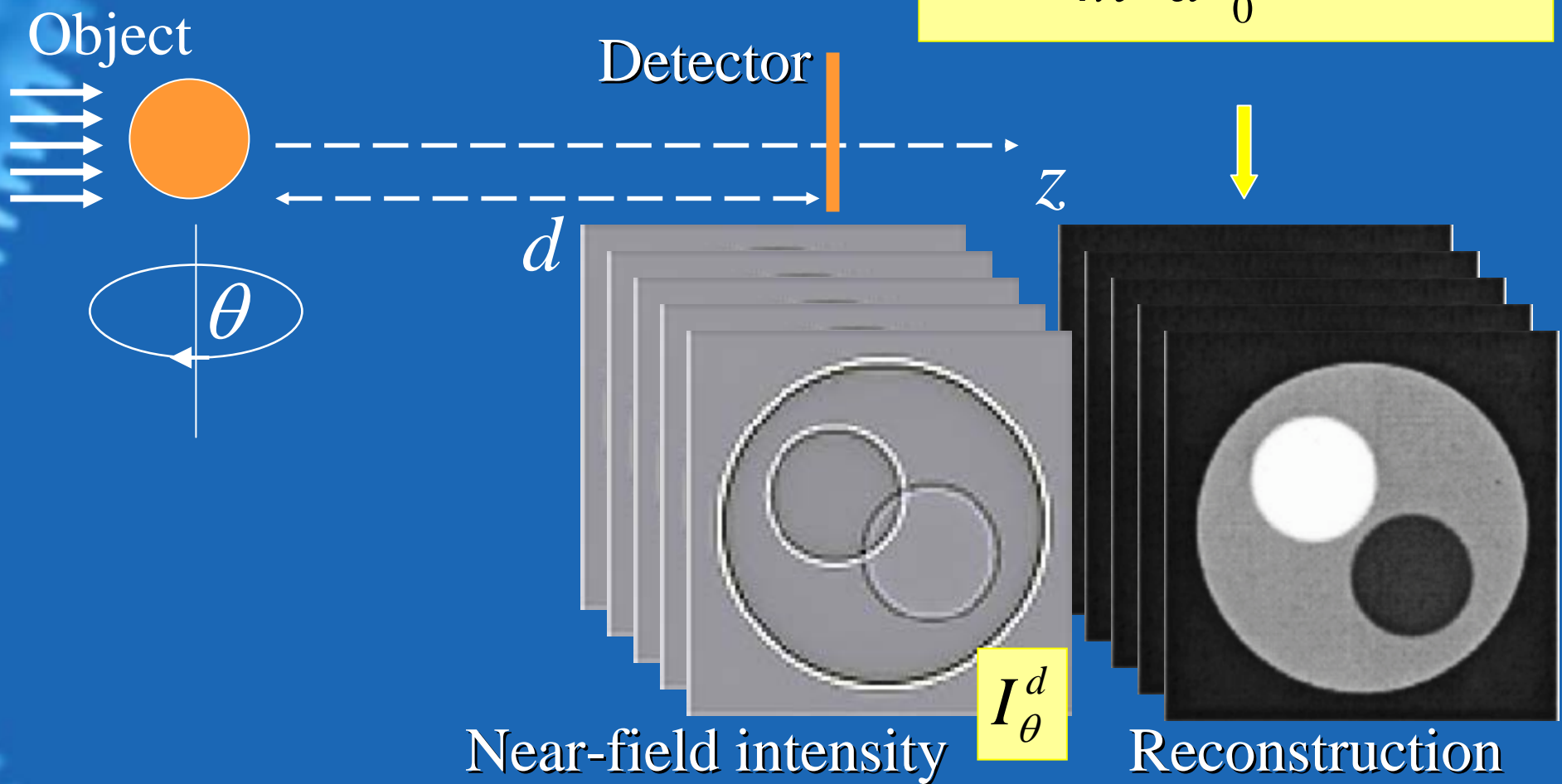


The fastest algorithm possible

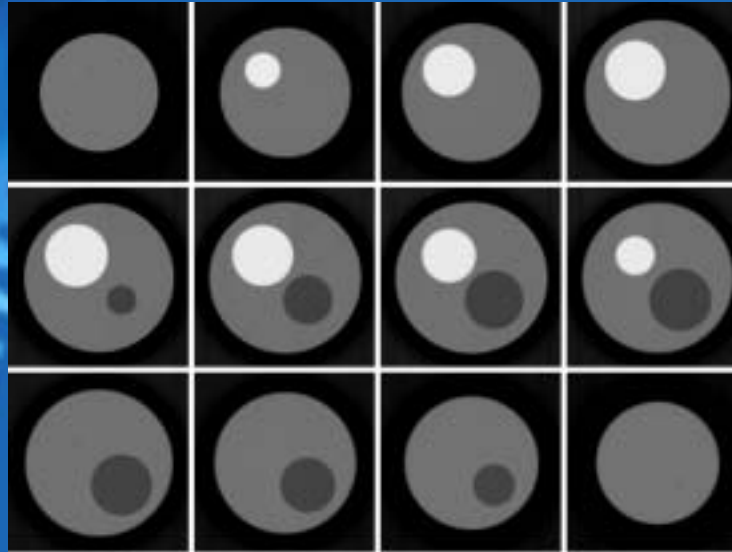
Phase object

$$g_\theta(x, y) = I_\theta^d / I_i - 1$$

$$f = \frac{1}{4\pi^2 d} \int_0^\pi q * * g_\theta d\theta$$



Phantom studies: polystyrene sphere



3D computer phantom

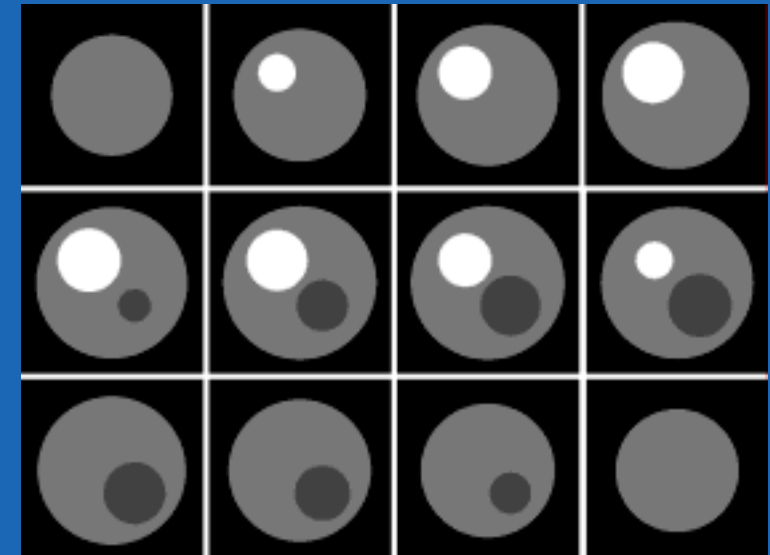


Phase-contrast
projections

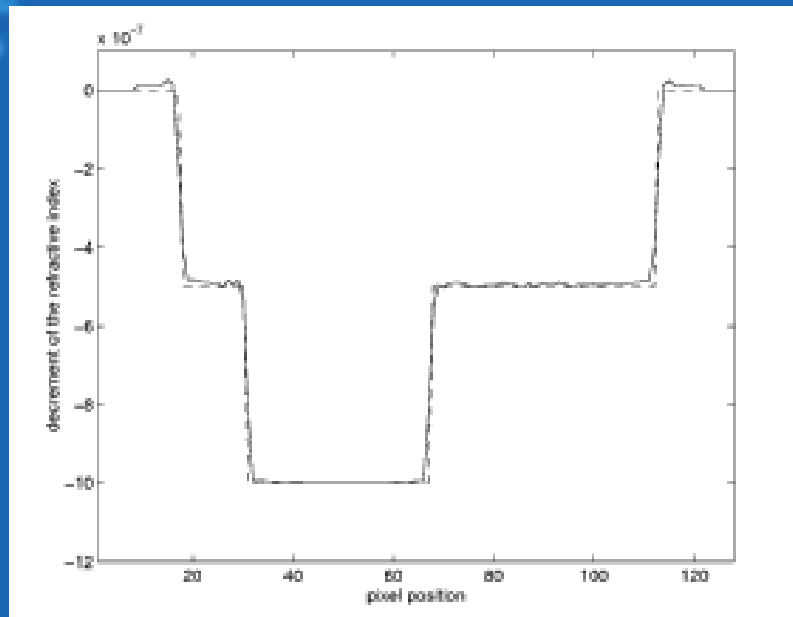
$$d = 2.5 \text{ cm}$$

$$\lambda = 0.1 \text{ nm}, \Delta = 1 \mu\text{m}$$

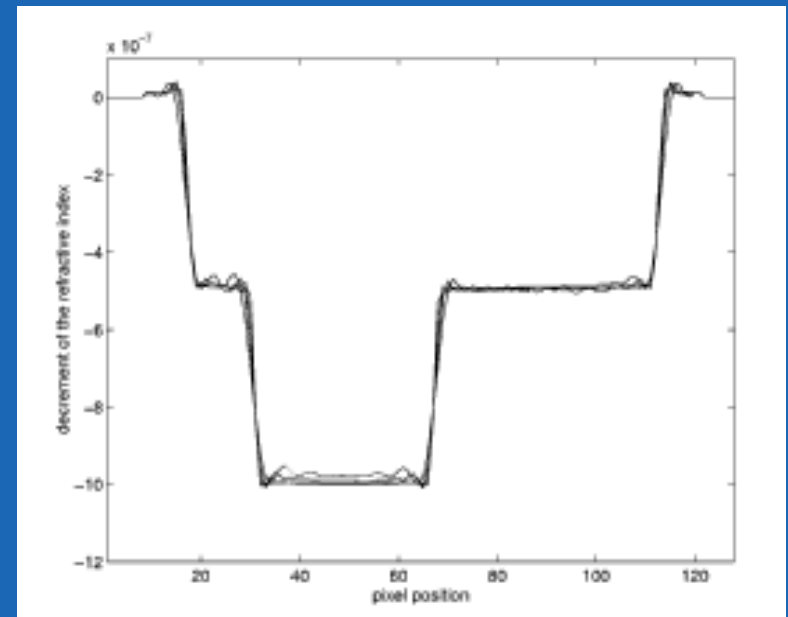
3D reconstruction



Quantification and the limits of the linear approximation

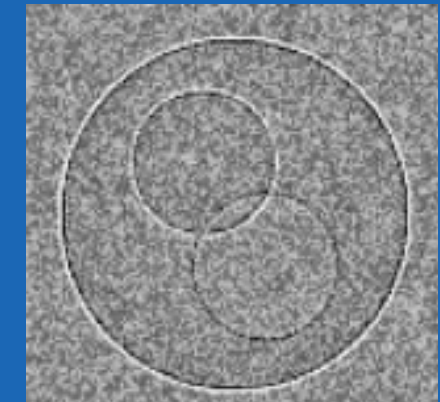
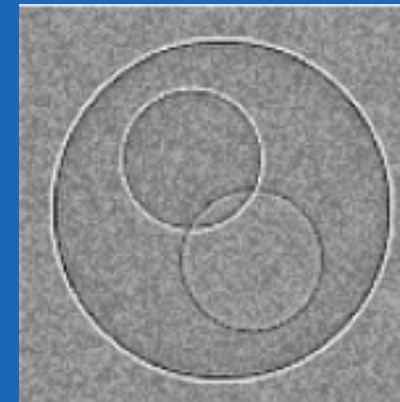
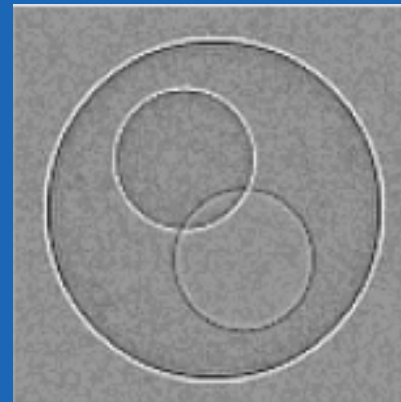


$$d = 2.5 \text{ cm}$$



$$1.5 < d < 20 \text{ cm}$$

Stability to noise

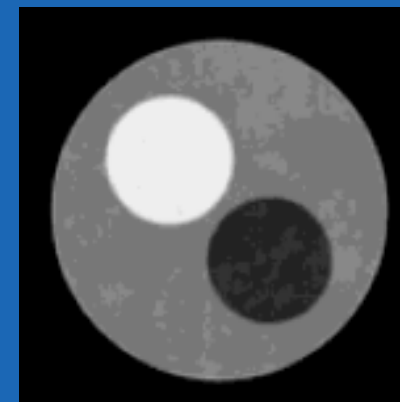
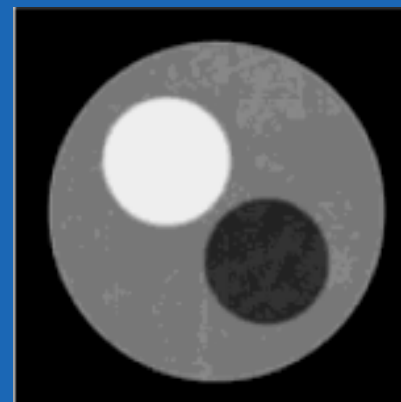


0%

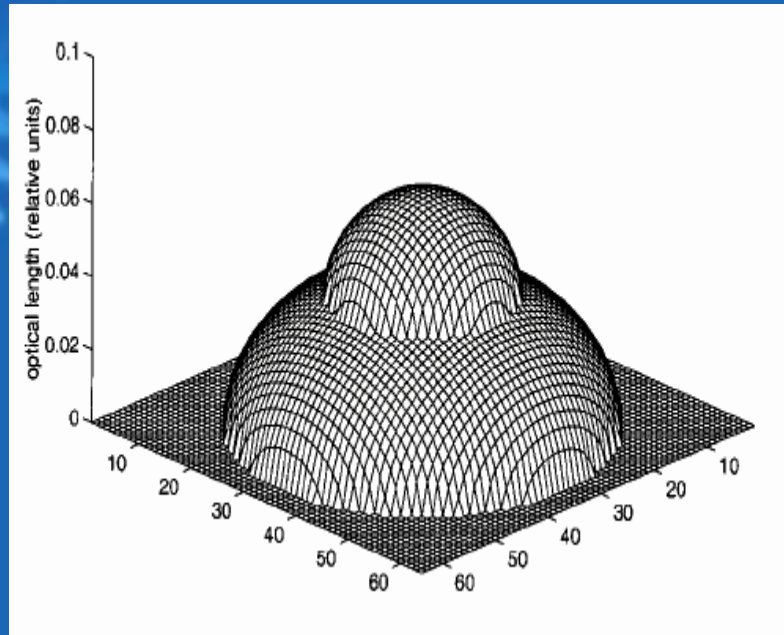
1%

2%

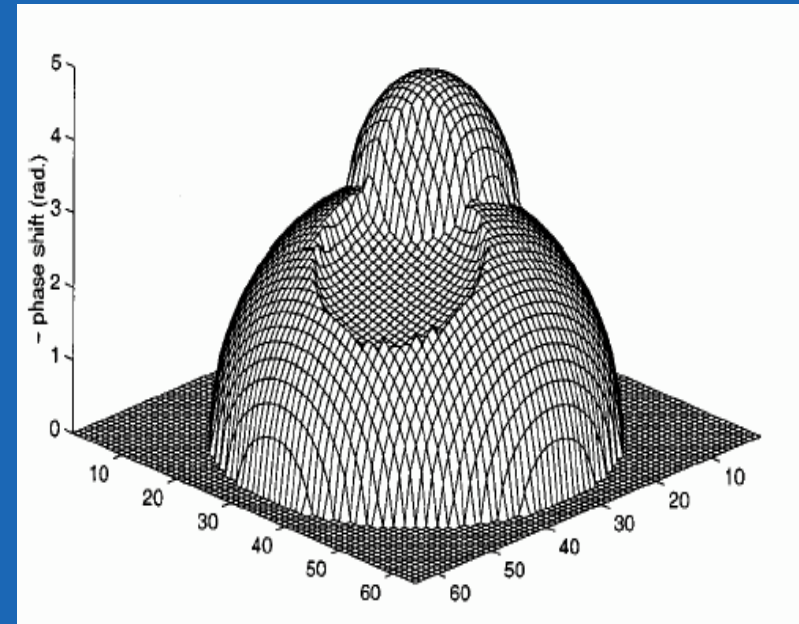
5%



Mixed phase and amplitude object



Absorption function $\mu/2$



Phase function φ

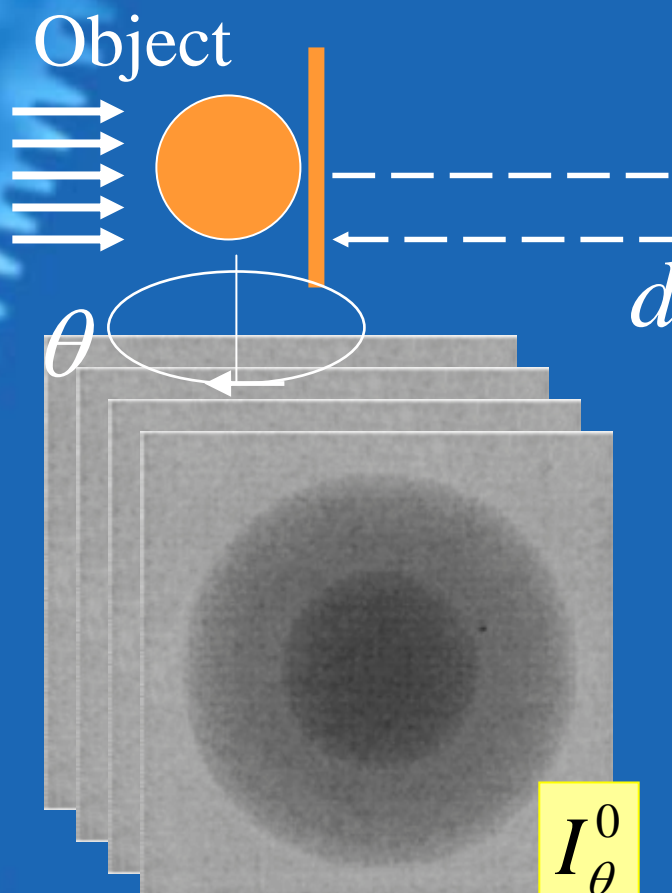
$$T(x, y) = e^{-\frac{1}{2}\mu(x, y)+i\varphi(x, y)}$$

Mixed phase and amplitude object

$$g_\theta(x, y) = I_\theta^d / I_\theta^0 - 1$$



$$f = \frac{1}{4\pi^2 d} \int_0^\pi q ** g_\theta d\theta$$

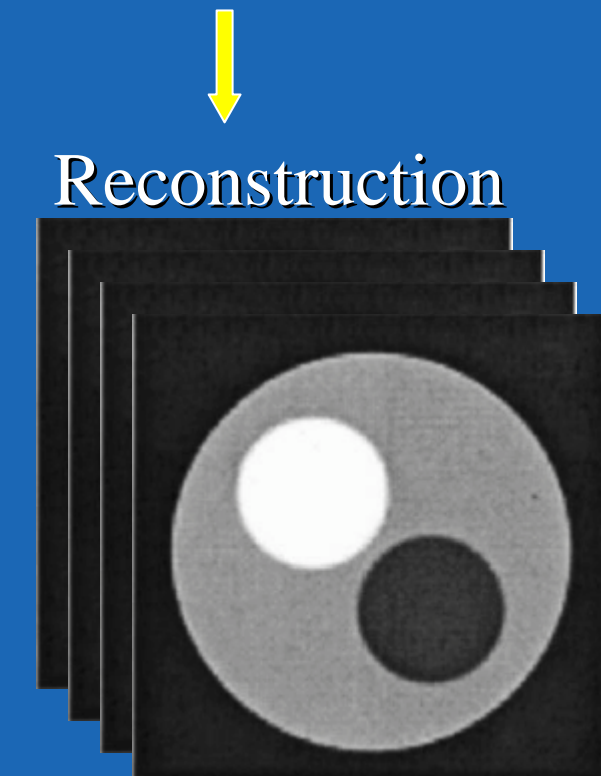


Contact intensity

Near-field intensity

$$I_\theta^0$$

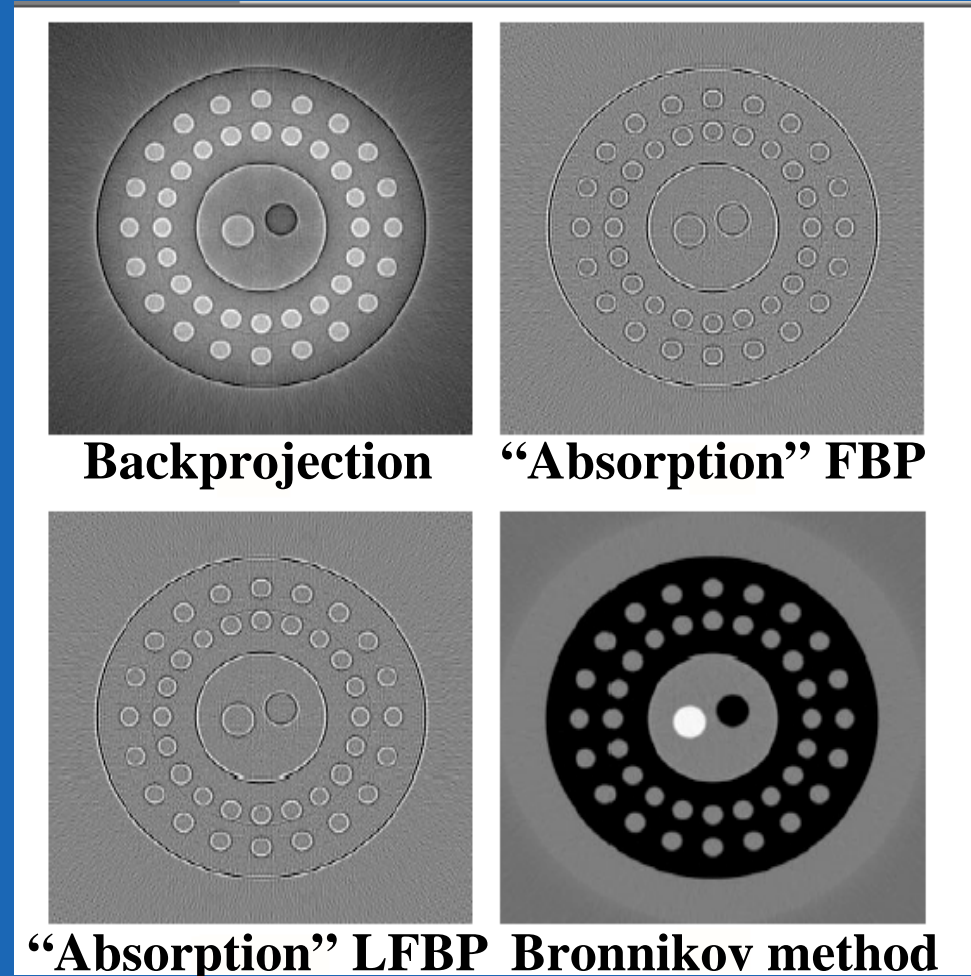
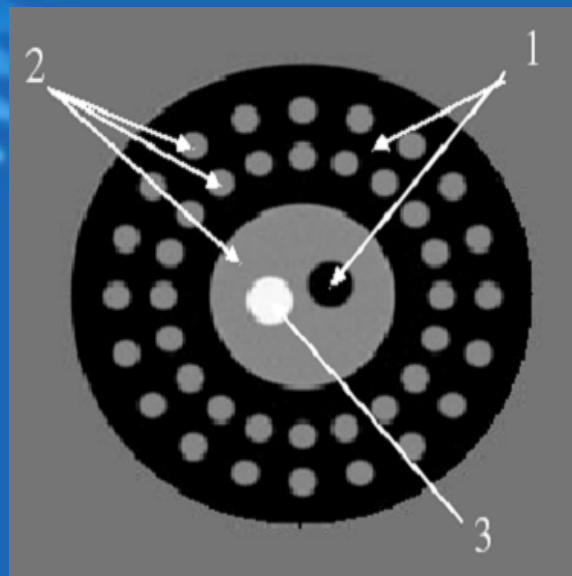
$$I_\theta^d$$



Reconstruction

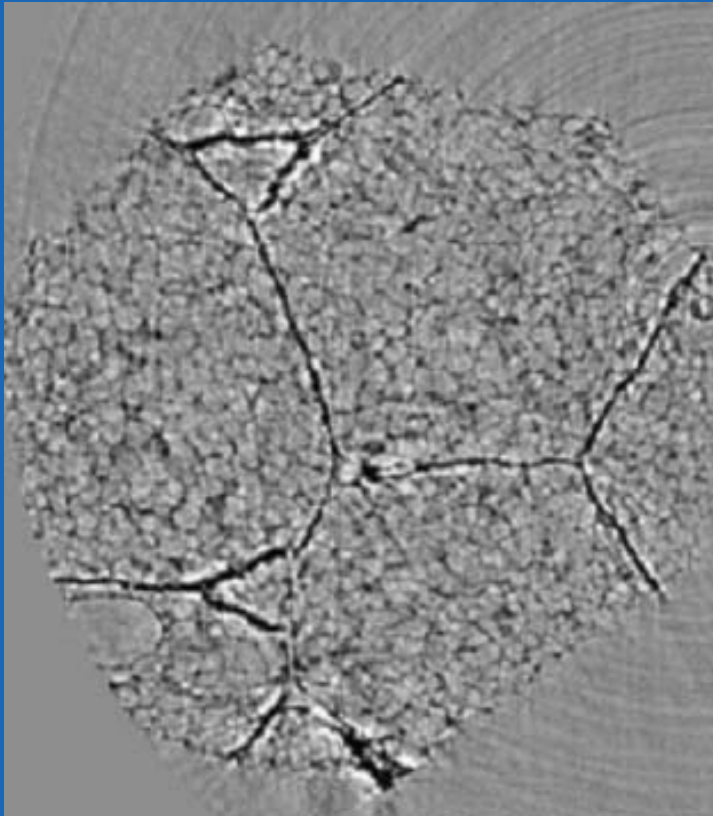
Comparison with heuristic methods

(Anastasio et al, PMB 2003)

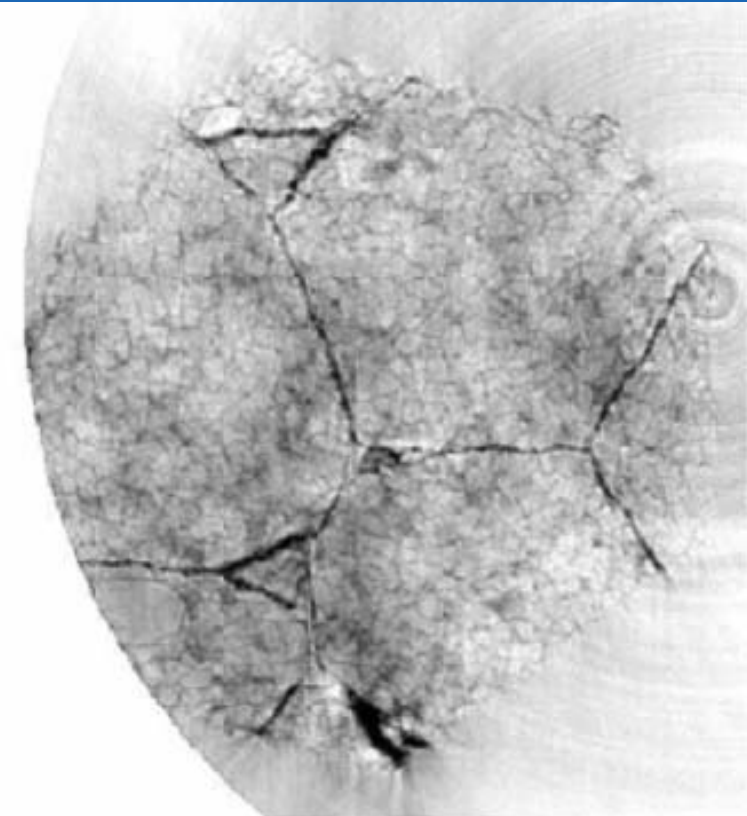


Polypropylene foam

(Schena et al; Elettra, 2004)

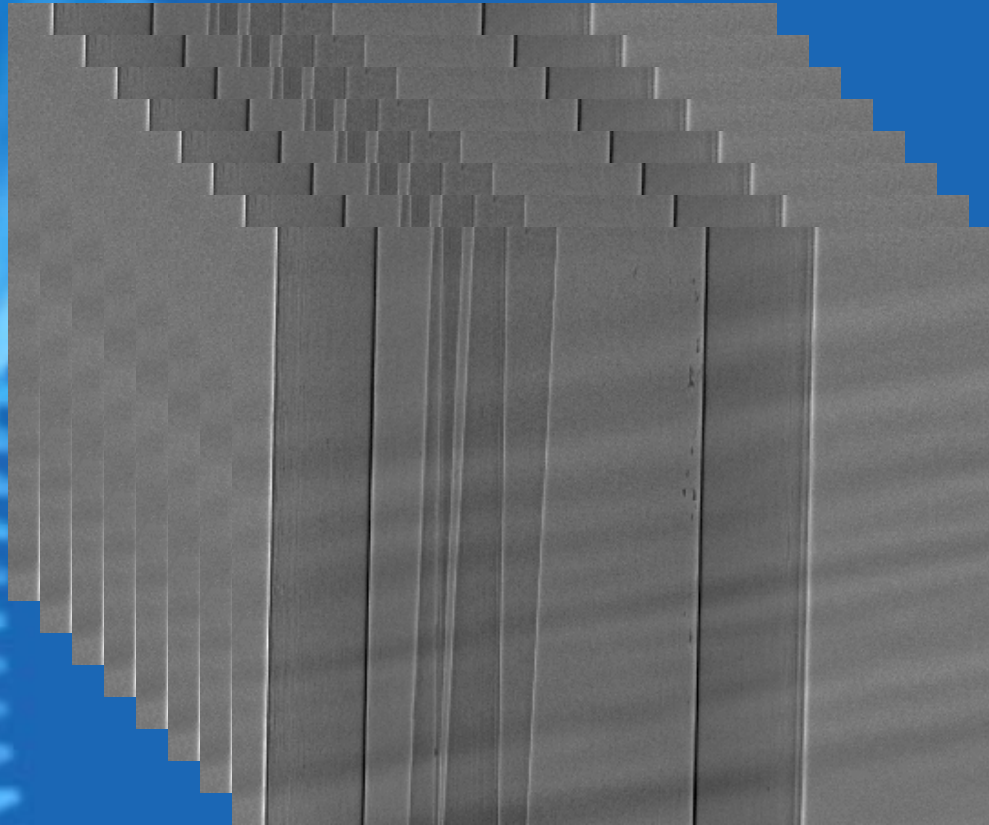


Conventional FPB



Bronnikov method

Polyethylene tube with polymer fibers (Groso and Stampaoni; SLS, 2005)



*721 projections; 15 cm distance sample detector; Energy=13.5 keV
Pixel size 1.75 microns*

Summary

- A fundamental theorem has been proved. This is the counterpart of the Fourier slice theorem used in absorption-based CT
- A fast image reconstruction algorithm has been implemented in the form of filtered backprojection (FBP)